

Origin of brown coloration in diamond

L. S. Hounsome and R. Jones

*School of Physics, University of Exeter, Stocker Road, Exeter EX4 4QL, United Kingdom*P. M. Martineau and D. Fisher
*DTC, Maidenhead SL6 6JW, United Kingdom*M. J. Shaw and P. R. Briddon
Physics Centre, School of Natural Science, Newcastle upon Tyne NE1 7RU, United Kingdom

S. Öberg

Department of Mathematics, Luleå University of Technology, SE-97187 Luleå, Sweden

(Received 12 December 2005; published 30 March 2006)

Measurements of the absorption spectra of brown natural type IIa diamond as well as brown nitrogen-doped CVD diamond are reported. These are largely featureless and increase almost monotonically from about 1–5.5 eV. It is argued that the brown coloration is due to an extended defect and not to a point defect. First principles modeling studies demonstrate that the spectra could be attributed to vacancy disks lying on {111} planes. Such disks are unstable above about 200 vacancies and should relax to dislocation loops in natural diamond. Hydrogen is shown to passivate the optical activity of the disks.

DOI: [10.1103/PhysRevB.73.125203](https://doi.org/10.1103/PhysRevB.73.125203)

PACS number(s): 61.72.Bb, 31.15.Ar, 31.15.Ew, 71.55.Cn

I. INTRODUCTION

A diamond may exhibit a range of colors due to different impurities and defects. Substitutional nitrogen, for example, leads to the familiar yellow color of high-pressure high-temperature (HPHT) synthetic crystals. Some natural diamonds and single-crystal chemical vapor deposition (CVD) diamonds are brown but in neither case has the origin of the color been established. This is despite significant interest stemming from the fact that high-temperature treatments can remove the brown color allowing the production of near-colorless gem quality stones.^{1–3}

We report here the absorption spectra of brown natural type IIa diamond and of single-crystal CVD diamond, grown at temperatures in the region of 800–900°C. The absorption coefficients of the natural diamond samples vary approximately as E^n (with n in the range 2 to 3) from energies around 1.0 eV up to the indirect band edge at 5.5 eV. The samples of brown single crystal CVD diamond have similar absorption spectra but display additional broad features that are described later. In neither case is there any evidence of an energy threshold above which the absorption begins. It appears that neutron irradiation or ion implantation can lead to an absorption spectrum similar to, if not identical to, that of brown natural type IIa diamond.⁴

The natural and single-crystal CVD diamond samples for which absorption spectra are reported here have different nitrogen contents. In the type IIa natural diamond samples the nitrogen concentration is below the detection limits. The CVD diamond material, although nominally type IIa, contains nitrogen at concentrations in the range 10^{16} – 10^{17} cm⁻³. This nitrogen is incorporated during the growth process along with significant amounts of hydrogen, the presence of which can be deduced, for example, from features in the infrared spectrum that have been attributed to hydrogen-

related defects. It is likely that defects involving nitrogen or hydrogen or both are responsible for the additional broad absorption features that are observed in the spectra of brown single-crystal CVD diamond material.

Brown color in natural type IIa diamond is believed to be a result of the presence of defects created by a naturally occurring process of plastic deformation, caused when a diamond experiences conditions of large nonhydrostatic pressure, in which dislocations are created (with densities of the order of 10^9 cm⁻²) and move through the crystal. It is currently not known whether the brown color results because of the presence of dislocations or because of otherwise undetected defects produced when the dislocations move through the crystal. This is the subject of current research.

It is known that as-grown brown single-crystal CVD diamond has not experienced the conditions required to produce extensive plastic deformation. This is supported by the fact that such material does not contain dislocations of the kind produced by plastic deformation. Such CVD material typically contains dislocations at much lower densities (of the order of 10^4 – 10^6 cm⁻²) than those in a brown type IIa natural diamond and in configurations indicating that they have been grown-in rather than being produced by deformation. These observations suggest that the brown color of such CVD diamonds are caused neither by its dislocation content nor by defect that are produced by the movement of such dislocations through a crystal during plastic deformation.

There are significant differences between the annealing characteristics of the different kinds of diamond. The absorption continuum disappears for irradiated material at 1400°C,⁵ and in the range 1400–1600°C for brown single-crystal CVD material.⁶ For brown natural type IIa diamond, however, temperatures above 2200°C are required to remove the absorption continuum.⁷ This suggests that either the stabilities of the defects responsible for the absorption con-

tinuum in for brown single-crystal CVD material and natural diamond are significantly different or the mechanism for its loss are different. In this paper we explore the possibility that the latter is the case, with hydrogen-containing defects present in the CVD samples playing a role in the removal of the absorption continuum caused by annealing.

There are four possible explanations for the absorption continuum. It may be due to point, line, areal, or volume defects. Such an absorption spectrum is unlike that due to point defects. Many of these display a sharp absorption edge followed by a vibronic broad peak, e.g., the well-known GRI spectrum due to a vacancy has a threshold at 1.67 eV.⁸ The defect that results when nitrogen substitutes for a carbon atom, possesses a broad absorption band due to transitions between a gap level and the conduction and valence bands but with a threshold around 2 eV.⁹ A threshold energy would imply that the defect introduced levels into the band gap of diamond whereas the observed continuum absorption would arise if the defect introduced levels which completely filled the gap. The absence of a threshold points to an extended defect being responsible for the brown coloration. We have previously reported the electronic structure of a shuffle dislocation,¹⁰ whose core consists of a line of dangling bonds leading to a broad band of states lying in the gap. These states could, in principle, explain the brown absorption. Although brown natural type IIa diamond has been found to contain dislocations¹¹ at densities of up to 10^9 cm⁻², the densities of dislocations in the samples of brown single-crystal CVD diamond discussed here are much lower and too low to account for the color. Moreover, the shuffle dislocation is predicted to be less stable than the glide dislocation, the core of which consists of reconstructed *sp*³ carbon bonds and is optically inactive.¹⁰ The greater stability of the glide dislocations suggests that they would be more prevalent than the shuffle dislocations which are therefore unlikely to be responsible for the brown color even in natural type IIa diamond.

It is likely that vacancies are involved in the centers responsible for the brown coloration because studies of the transformation of brown to colorless natural brown diamond¹ find that vacancy-nitrogen defects are formed during the anneal. Annealing brown diamond to remove the color can cause changes in the positron decay curves that are consistent with changes in the content of vacancy-related defects and voids.^{12,13}

We have previously investigated the structure and optical properties of clusters of up to 14 vacancies.¹⁴ These introduce a number of levels into the band gap. A single multi-vacancy cluster could not explain the brown coloration as a threshold is then to be expected. On the other hand, an ensemble of clusters of different sizes may not exhibit a threshold but would be expected to give an absorption pattern which varied from sample to sample reflecting a different relative concentration of the clusters. Moreover, during the anneal, the less stable ones would dissolve leaving the more stable ones. The latter would lead to an absorption spectrum with structure contrary to observations.

We show here that the absorption pattern produced by the π -bonds in an extended vacancy disk is strikingly similar to that found experimentally, notably the absence of a threshold

and the absorption spectrum is featureless and varies like E^2 in the mid-gap region. Moreover, the formation energy per vacancy in the disk is much lower than that of small vacancy clusters of size 1–14 vacancies.¹⁴ It is shown later that as the size of vacancy clusters increase their formation energy per vacancy decreases, that is they become more stable. This suggests that disks could be formed through an aggregation process where smaller vacancy clusters dissolve by emitting vacancies allowing disks to grow as in Oswald ripening. This would require temperatures $>700^\circ\text{C}$, where the vacancy is mobile.

It has been described above how CVD and natural diamond differ in the conditions they have experienced, which indicates that the formation conditions for any defects will be different. While this difference may be expected to lead to different defects being prevalent, it is possible for the same defect to form via different routes.

During high growth rate CVD processes, the growing surface can become rough and stepped and then rapidly covered to leave small voids or clusters of vacancies. The high growth temperature would allow the incorporated vacancies to become mobile, re-organizing by dissolution into vacancy disks, with a consequent energy reduction. Dislocations are known to release vacancies during movement by climb or glide, and the energy necessary for such movement could occur during plastic deformation. The result is the same free single vacancies, but from a different source. It would be expected that mobile vacancies then follow a route of dissolution and reformation into vacancy disk, like that in CVD diamond.

We describe in the next section the experimental absorption spectra for a wide range of samples of natural and CVD brown diamond. In Sec. III, we explain the theoretical method used and report our results and finally, in Sec. IV, we give our conclusions.

II. ABSORPTION SPECTRA OF BROWN DIAMOND

The set of natural type IIa diamond samples displayed depths of brown color covering the range found in nature. Windows were polished on opposite faces of these samples to allow spectra to be acquired and to minimize effects due to surface scattering. Sample thicknesses ranged between about 1.5 and 4.0 mm.

The CVD samples were grown homoepitaxially on {100} type Ib HPHT-grown substrates using microwave plasma CVD with nitrogen added to the process gases. The substrates were subsequently removed and the resulting plates of a CVD diamond were polished into parallel-sided plates with a thickness of approximately 1.5 mm. Absorption spectra were acquired at room temperature using a Perkin Elmer Lambda 9 ultraviolet/visible/near infrared spectrophotometer with a circular aperture of 2.0 mm diameter defining the measurement region.

The absorption spectra of a representative samples of brown single-crystal natural and CVD diamond, in the visible and ultra-violet, is shown in Fig. 1. A total of 32 natural IIa and 4 samples of CVD diamond were investigated and all displayed a similar absorption profile. It is to be noted that

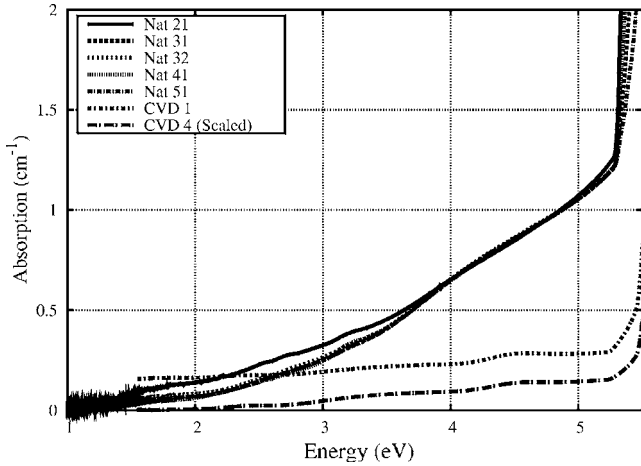


FIG. 1. Experimentally measured absorption spectra of five natural type IIa crystals and two samples of single crystal CVD grown brown diamond. The natural stones exhibit a featureless continuous absorption with no evidence of any threshold. The CVD samples show in addition some broad peaks which may be related to point defects. The absorption coefficient of CVD-4 has been multiplied by 0.01 for ease of comparison.

the absorption spectra are almost featureless and increase almost monotonically with energy. In some cases, peaks due to nitrogen related impurities at 4.5 eV⁹ can be seen together with two unidentified defects which absorb at ~ 2.5 and ~ 3.4 eV. Figure 1 shows that in all the samples investigated the same underlying continuum is present strongly suggesting there is a single defect responsible and not a number of different defects with different levels which combine to give an absorption continuum varying as E^2 or E^3 . In the latter case, we would expect differences in the populations of defects in the different samples and hence a different spectrum for each sample.

III. THEORETICAL ABSORPTION SPECTRA OF VACANCY DISKS

A. Method

We carry out local density functional calculations for the structure and dielectric constant of a vacancy disk embedded in a large unit cell using the AIMPRO code.¹⁵ Hartwigsen, Goedecker, and Hutter¹⁶ pseudopotentials and Gaussian s , p , and d basis sets are used to eliminate core electrons and describe valence electronic wave functions, respectively. Vacancy disks are created in 40 and 80 atom cells. The separation between the disks in different cells is then 20 and 40 atomic layers, respectively. The unit cell Brillouin zones are sampled with a Monkhorst-Pack grid of \mathbf{k} -points.¹⁷

The absorption coefficient is related to the complex dielectric constant of the cell by $(4\pi/\lambda)\text{Imag.} \sqrt{(\epsilon'_1 + i\epsilon''_2)}$. Here, l denotes a principal value of the dielectric tensor and $\epsilon'_l, \epsilon''_l$ are its real and imaginary parts. The imaginary part of the dielectric constant, in the long-wavelength dipole approximation, is given by¹⁸

$$\epsilon_2^l(E) = \frac{4\pi e^2}{\Omega} \sum_{c,v,\mathbf{k}} |\langle \Psi_{\mathbf{k}}^c | \mathbf{r}^l | \Psi_{\mathbf{k}}^v \rangle|^2 \delta(E_{\mathbf{k}}^c - E_{\mathbf{k}}^v - E) \quad (1)$$

where Ω is the unit cell volume, and $|\Psi_{\mathbf{k}}^{v,c}\rangle$ are valence and conduction states, with energies $E_{\mathbf{k}}^{v,c}$, respectively. The sum over \mathbf{k} includes the full Brillouin zone, which we sample with a regular Monkhorst-Pack grid containing 3000 k -points for bulk, and 500–1500 k -points for supercells containing defects. The δ function has the effect of broadening the calculated points to form a continuous spectrum. The value must be chosen carefully as too large a broadening can remove features from the spectrum, but too small a broadening renders the information unusable. In general, some small fraction of the bandgap is a good compromise. Here we use a polynomial broadening of 0.8 eV. In a solid, the matrix element of \mathbf{r} is evaluated using:¹⁹

$$\langle \Psi_{\mathbf{k}}^n | \mathbf{r} | \Psi_{\mathbf{k}}^i \rangle = \frac{1}{i\omega m} \langle \Psi_{\mathbf{k}}^n | \mathbf{p} | \Psi_{\mathbf{k}}^i \rangle + \frac{1}{\hbar\omega} \langle \Psi_{\mathbf{k}}^n | [V_{nl}, \mathbf{r}] | \Psi_{\mathbf{k}}^i \rangle \quad (2)$$

where V_{nl} is the nonlocal part of the pseudo-potential. The real part of the dielectric function is subsequently obtained through a Kramers-Kronig (KK) transformation. More involved theories of dielectric functions have been developed for semiconductors, to describe effects beyond LDA,²⁰ beyond the long-wavelength limit,²¹ and beyond the independent particle limit,^{21,22} but they are currently too computationally intensive to be applied to anything other than bulk materials.

The local density functional theory used here also leads to a well known underestimate of the gap. We find a gap of 4.2 eV compared with an experimental value of 5.5 eV. There are two simple methods by which this can be corrected. The first is a rigid upward shift of the levels lying above the valence band top, E_v . However, this method cannot lightly be applied to a defect which introduces both occupied and unoccupied gap levels for in this case, it seems unlikely that the occupied states should be rigidly shifted. Such a shift would disturb the ground state structural properties predicted by the theory. Instead, we prefer to scale the energy levels lying above E_v by a factor of 1.3. Applied to bulk diamond, this brings both the calculated indirect and direct band gaps at 4.22 and 5.66 eV into agreement with experimental data,²³ shown in Fig. 2.

B. Theoretical results

The infinite vacancy disk is created by removing two planes of atoms as shown in Fig. 3. These lie on aB planes of the normal $AaB\beta C\gamma$ (111) stacking sequence of diamond and their removal leads to dangling bonds lying parallel to [111] on each internal surface. The collapse of this vacancy disk, when the two planes fuse, does not lead to an intrinsic stacking fault as this requires the removal of $A\alpha$ planes. For the aB disk, fusing the two surfaces could be accompanied by a $a/2(110)$ shear and this leads to a perfect dislocation loop with this Burgers vector.

The formation energy per vacancy is 1.46 eV in both the 40 atom and 80 atom cells. These energies are to be compared with 5.96 eV for an isolated vacancy studied using a

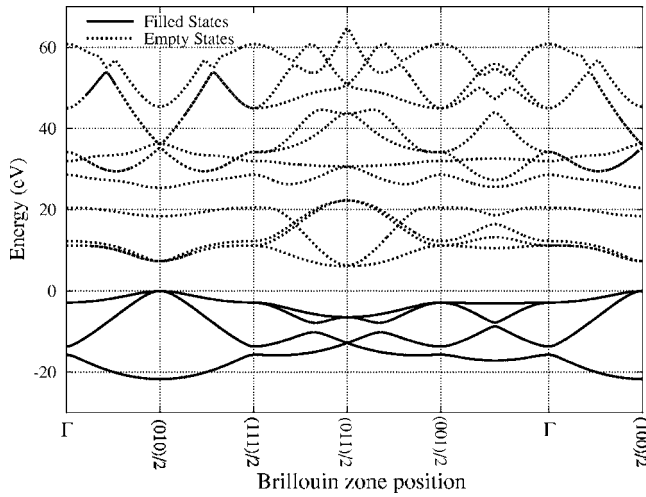


FIG. 2. Band structure of bulk diamond, calculated in a 2 atom cell. The energies of states above E_v are scaled by 1.3 to reproduce the direct and indirect bandgaps at 5.5 and 7.3 eV, respectively. The valance band top is set to 0 eV.

quantum Monte Carlo technique²⁴ and 7.17 eV in density functional theory. The most stable multivacancy cluster found previously is a cluster of 14 vacancies with formation energy 2.35 eV per vacancy.¹⁴ The reduction in formation energy with the size of the vacancy cluster is due to the elimination of some of the dangling bonds rather than stabilization of the surfaces of the cluster through reconstruction. However, this is not the case for a vacancy disk. Here *all* dangling bonds are eliminated through the Pandey reconstruction²⁵ which leads to lines of π -bonds lying along $[1\bar{1}0]$, and a reduction in energy of 0.52 eV per vacancy compared to a disk with unreconstructed surfaces. The length of the π -bond is 1.426 Å and close to that found in graphite (Fig. 4).

The band structure, shown in Fig. 5, demonstrates that the band gap is completely filled with states and that the top of the occupied π -band is degenerate with the bottom of the

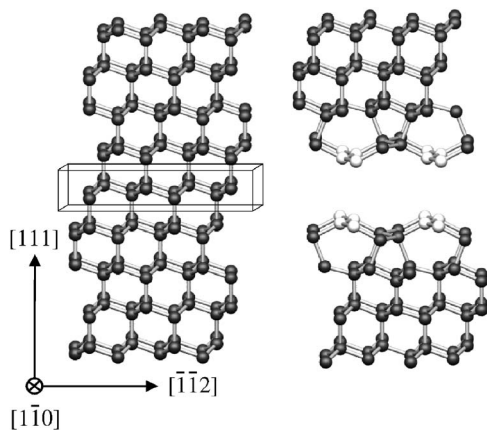


FIG. 3. Illustration of the removal of a $\{111\}$ double plane (boxed) in bulk diamond and the subsequent surface rebonding leading to a vacancy disk with chains of π -bonded atoms along $\langle 1\bar{1}0 \rangle$, shown in white for clarity.

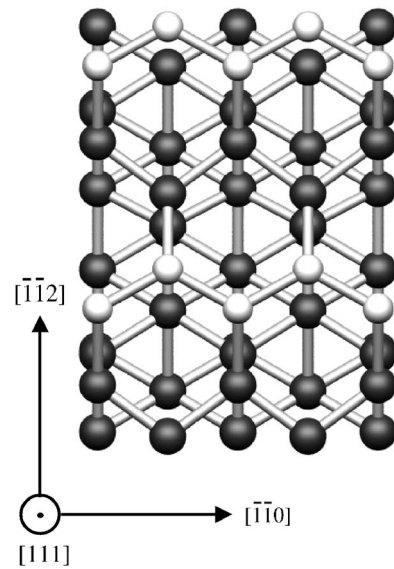


FIG. 4. View of the $\{111\}$ plane with a (2×1) Pandey chain reconstruction. The π -bonded atoms are smaller and colored white for clarity. The length of the π -bond is 1.426 Å.

empty π^* -band. Thus it can be anticipated that the absorption will be continuous without any threshold. However, it remains to show that the absorption is featureless and to determine its dependence on energy.

We found the diagonal components of the dielectric tensor for the planar defect along the $[111]$, $[1\bar{1}0]$, $[2\bar{1}\bar{1}]$ directions. The largest component lies in the (111) plane as indeed is found for graphite. We then find the average values of the dielectric constant and the corresponding optical absorption coefficient, shown in Fig. 6 and on a log-log plot in Fig. 7. One notes that the absorption is featureless in the range

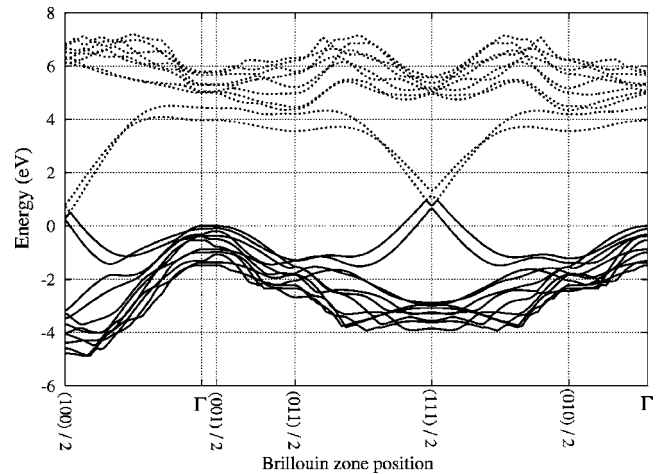


FIG. 5. Band structure of the vacancy disk in a 40 atom cell. The valance band top at Γ is set to 0 eV and the higher energy levels are scaled by 1.3 as described in the text. Note the absence of any pronounced gap in the spectrum suggesting a featureless absorption spectrum. Dashed lines are unoccupied levels, while solid lines show filled levels. The center of the Brillouin zone is marked Γ , and other \mathbf{k} -points denoted with their positions relative to the primitive unit vectors of the Brillouin zone of the 80 atom cell.

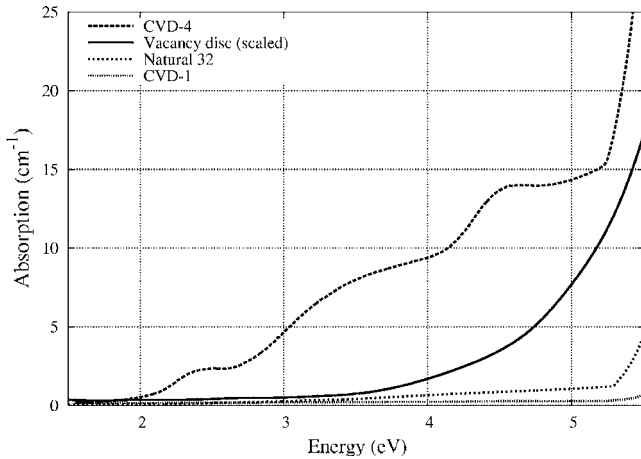


FIG. 6. Absorption of natural and CVD grown brown diamond compared to absorption of $\{111\}$ vacancy disk in an 80 atom cell. The absorption of the vacancy disk has been multiplied by a factor of 0.000 25 for clarity.

1–5 eV as indeed is the experimental spectrum and the energy dependence of the absorption is very similar to the more transparent CVD-1 sample in the mid-gap region. Supplementary absorption in CVD-4 is due to additional defects including nitrogen. Now, the expression for the dielectric constant above takes only direct electron-hole transitions into account and hence the large rise in absorption at 5.5 eV for diamond, due to indirect excitations and exciton effects, is not reproduced. In addition, the semi-metallic character of the infinite vacancy disk results in an absorption coefficient

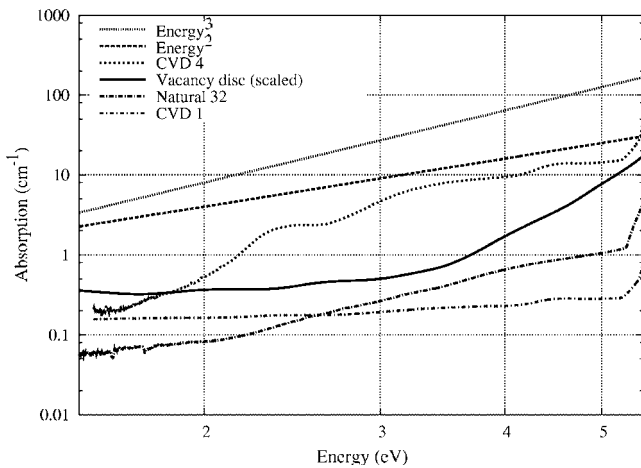


FIG. 7. Log-log plot of absorption coefficient of natural type IIa brown diamond, and two samples of nitrogen doped CVD diamond along with lines E^2 and E^3 which indicate the energy dependence of the absorption. The calculated absorption coefficient for a $\{111\}$ vacancy disk in an 80 atom cell, multiplied by a factor of 0.000 25, is also shown. Note that it follows closely the absorption of the more transparent CVD-1 sample. The theoretical spectra below 2 eV and above 5 eV are not reliable (see text). The broad band at 4.6 eV in CVD-4 is attributed to substitutional nitrogen but the bands at 2.48 and 3.39 eV are unaccounted for and may be related to other defects not detected in natural IIa brown and which are less prominent in CVD-1.

diverging at low energies.²⁶ A finite disk would possess a small gap between occupied π -bonding and empty antibonding states leading to an absorption coefficient which vanishes with energy. However the vacancy disk clearly leads to an absorption spectrum consistent with experiment on CVD-1, although the natural diamond may have additional centers.

An important finding is that the calculated absorption coefficient found in the 80 cell is roughly a factor of half that found in the 40 atom cell where the density of vacancies is twice as large. Thus our absorption coefficient scales with this fraction. This allows us to calibrate the absorption with the sp^2/sp^3 fraction or vacancy density. We find an absorption coefficient at 2.5 eV of 0.05 cm^{-1} for a vacancy concentration of $\sim 1 \text{ ppm}$ or $1.52 \times 10^{17} \text{ cm}^{-3}$. This is comparable with an extrapolation of experimental data on poor quality CVD material.²⁷ Thus we can deduce that there are about 10^{17} vacancies in the CVD-1 diamond whose absorption is shown in Fig. 7 if all the absorption were due to disks. It is to be expected that the π -bonds lead to vibrational modes in the 1500 cm^{-1} regions and indeed our calculations find a Raman active mode at 1494 cm^{-1} . This is close to one observed around 1540 cm^{-1} in CVD material.³ Similar modes must be present in natural brown diamond if the vacancy disk model is correct.

We now discuss possible mechanisms for the loss of the brown coloration. Recent experiments²⁸ show that the transformation of brown to colorless CVD brown diamond is accompanied by the growth of a broad C-H band around 2900 cm^{-1} . This frequency is close to the C-H stretch mode on a (111) surface,²⁹ which occur at 2838 cm^{-1} . The question arises whether hydrogen could passivate the optical activity of the disk.

Figure 8 shows the hydrogenated disk. Here a layer of H atoms passivates the surface dangling bonds, and it is found that the stable disk has a (1×1) surface. The carbon-hydrogen bond length here is 1.11 \AA and the separation of the C atoms across the disk is 4.02 \AA . The band structure in Fig. 9 shows that hydrogen has now eliminated all states from the band gap of diamond. The formation of C-H bonds provides an explanation for the loss of the brown coloration in CVD diamond. However, the lack of hydrogen in natural brown diamond requires an alternative explanation for the loss of the brown coloration.

Large vacancy disks would not be stable against collapsing to produce a perfect dislocation loop. If one of the surfaces was displaced towards the other by $a(110)/2$, then the fault would be eliminated but a perfect dislocation loop with this Burgers vector b would be formed. According to previous theory and electron energy loss spectroscopy, such loops are likely to be optically inactive.¹⁰ The energy of a collapsed disk of radius r , according to elasticity theory³⁰ is,

$$\sim \frac{\mu b^2 r}{2[1 - \nu]} (\ln(4r/b) - 1),$$

Here μ and ν are the shear modulus and Poisson ratio of diamond. We find the energy of the dislocation loop to be less than that of the vacancy disk for loops of radius greater

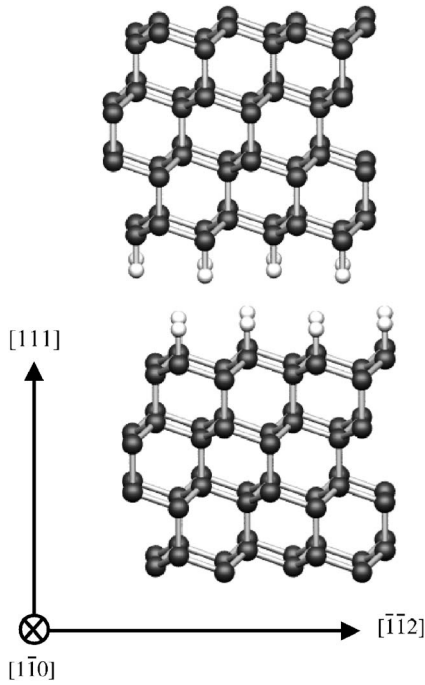


FIG. 8. Hydrogenation of the [111] surfaces, passivating the π -bonds. Hydrogen atoms shown in white.

than about 12 Å containing about 200 vacancies.

The vacancy disk considered so far consists of the removal of just two atomic layers. It is possible to imagine that further pairs of atomic planes are removed and each pair replaced by a single plane of graphene. As the numbers of removed and added atoms are the same, the number of vacancies is unaltered. Diamonds with graphitic inclusions having this orientation have been reported.³¹ Furthermore,

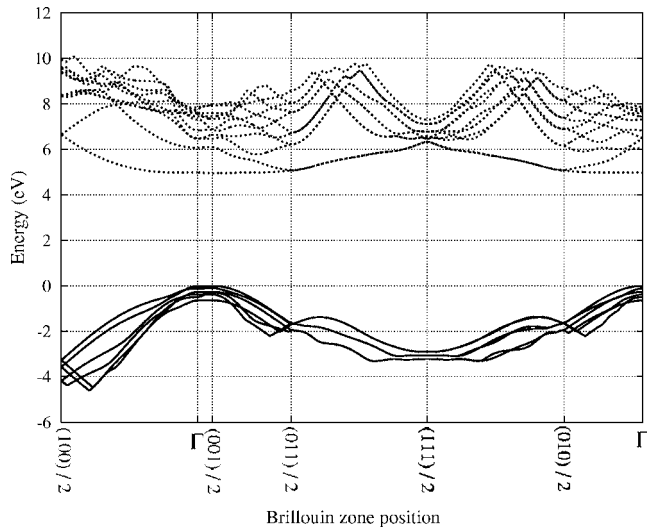


FIG. 9. Band structure of the hydrogen terminated {111} vacancy disk. It can be clearly seen that the band gap is cleared of states, allowing no optical absorption in the visible range. Valence band top set to 0 eV. Dashed lines are unoccupied levels, while solid lines show filled levels. Brillouin zone points denoted as before. Energy levels above the top of the valance band are scaled by a factor of 1.3.

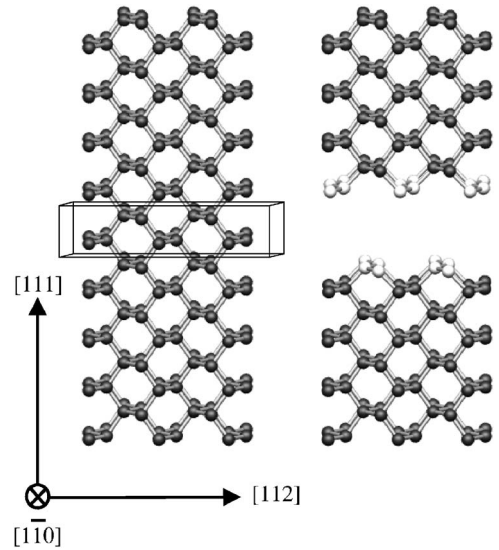


FIG. 10. Illustration of the removal of a {110} double plane (boxed) in bulk diamond and the subsequent surface rebonding leading to a vacancy disk with chains of π -bonded atoms along [001], shown in white for clarity.

transmission electron microscopic observations of brown natural type IIa diamond report features possibly due to graphitic inclusions.³² However, the formation energy of a single plane of graphene lying inside the vacancy disk is 1.72 eV per vacancy which is higher than the 1.46 eV formation energy per vacancy found above for the vacancy disk. Clearly, the single plane of graphene is unstable, however, this may not be the case for larger graphitic inclusions bearing in mind that graphite is more stable than diamond.

It would be possible for a surface of π -bonded atoms to form on the facets of a sufficiently large octahedral void, in this case the 8 faces would lie on the set of (111) planes. Preliminary investigations of a void of 35 vacancies arranged in this pattern give a formation energy of 1.85 eV per vacancy which is quite stable. The facets of this void were too small to allow formation of Pandey chains or delocalised π -bonds so evidence for bandgap optical absorption is still lacking, but larger voids would be computationally expensive to model.

A study has also been made of a vacancy disk lying on the {110} plane, which naturally forms a chain of π -bonded atoms when a double layer is removed,³³ shown in Fig. 10. The disk is created in a cell of 40 atoms with a separation between disks of 10 atomic layers.

The formation energy is higher than the disk on a {111} plane, at 1.71 eV per vacancy. The band structure shown in Fig. 11 displays a gap at ~ 3 –5 eV above the valance band top which would be expected to lead to a feature in the absorption spectra, and this is confirmed by further calculations, which demonstrate a dip in absorption around 4 eV, illustrated in Fig. 12. Thus it unlikely that these disks are present in appreciable numbers.

IV. CONCLUSIONS

We have shown that the absorption spectrum of natural type IIa single crystal brown diamond, and several samples

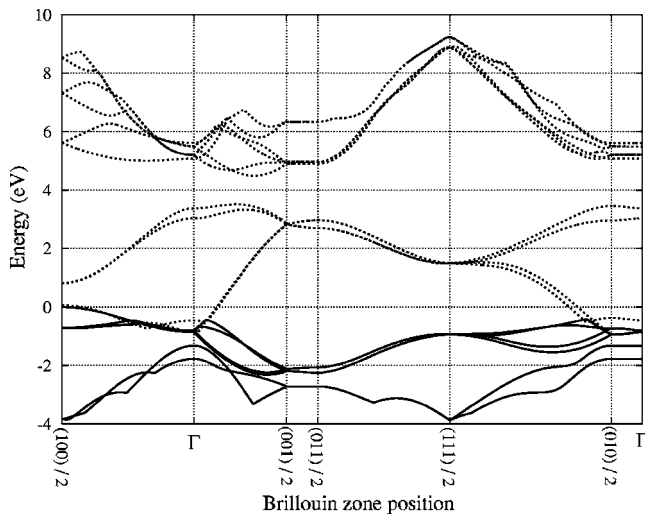


FIG. 11. Band structure of an infinite vacancy disk on the $\{110\}$ plane. The break in levels in the region of the top of the bulk band gap, leads to a nonfeatureless absorption spectrum. Dashed lines are unoccupied levels, while solid lines show filled levels. Brillouin zone points denoted relative to the primitive unit cell. Energy levels above E_v are scaled by a factor of 1.3.

of brown single crystal nitrogen doped CVD diamond, exhibit the same almost featureless absorption pattern, varying between E^2 and E^3 , which suggest that a single defect is responsible. Density functional calculations of vacancy clusters show that the most stable cluster found is a vacancy disk lying on $\{111\}$ planes for disks smaller than about 200 vacancies. The stability of the disk is due to the elimination of

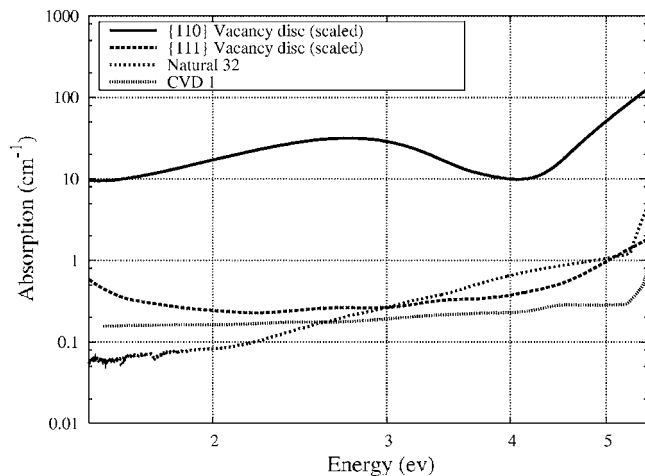


FIG. 12. The calculated optical absorption of a vacancy disk on the $\{110\}$ plane scaled by a factor 0.0025 for comparison, compared to the disk on the $\{111\}$ plane (scaled by a factor 0.000 25) and one natural and one CVD sample. Absorption from the $\{110\}$ disk clearly shows several features such as a broad band at ~ 2.8 eV and a dip in absorption around 4 eV where there are fewer band gap levels.

dangling bonds through the formation of π -bonded chains similar to the (2×1) reconstruction of the $\{111\}$ surface. The absorption coefficient of the disk exhibits the same featureless absorption profile as seen experimentally for brown diamond. Moreover, the highest local vibrational mode of the disk at 1496 cm^{-1} is close to a band detected experimentally at 1540 cm^{-1} in brown CVD diamond. We, therefore, identify $\{111\}$ vacancy disks as a likely candidate for the origin of the brown coloration, at least in the CVD-1 sample. In natural diamond, the experimental absorption bands vary more dramatically with energy which may reflect the presence of other vacancy centers. It may be that octahedral voids of vacancies having $\{111\}$ surfaces could also explain the brown color and these could also account for the very long 400 ps lifetime detected by positron annihilation in brown diamond.^{12,13} It is known that growth of Si by the Czochralski process introduces voids or “crystal orientated particles” which are vacancy clusters with $\{111\}$ surfaces up to $0.1 \mu\text{m}$ in size although the surfaces appear to be oxidized.³⁴

The band structure of the $\{111\}$ vacancy disk is quite distinct from that of the ideal 2×1 (001) diamond surface, where again a reconstruction leading to π -bonding occurs. However, in this case the π -bonds do not overlap appreciably, and lead to only narrow π bands and π^* bands lying within the gap, of width less than 2 eV, and separated by ~ 1.5 eV.³⁵ To achieve very broad π and π^* bands, separated by a narrow gap, it is necessary for the π -bonds to be connected together in for example chains or as in a graphene sheet. Only in this case, will the optical properties approach those of brown diamond. Discs lying on $\{110\}$ planes also do not exhibit the broad π and π^* bands which completely fill the gap and would not show the characteristic absorption of brown diamond.

Two mechanisms for the loss of the brown coloration upon annealing are investigated. In one, the surface of the disk is passivated with hydrogen and this could explain the growth of vibrational bands around 2900 cm^{-1} detected after the transformation of brown CVD diamond.²⁷ It is interesting to note that there is an analogy with hydrogen platelets in Si which are formed by proton implantation which also lie on $\{111\}$ planes although in this case the planes are pushed apart by hydrogen molecules.^{36,37} Secondly, the collapse of a large disk, and the formation of an optically inactive dislocation, is found to be energetically favorable for disks containing more than about 200 vacancies. Such a mechanism might account for the transformation of brown natural diamond although it is unclear whether the disks are growing and then become unstable, or the activation barrier to the collapse and the formation of a dislocation loop are overcome at temperatures around 2000°C .

ACKNOWLEDGMENTS

We thank U. Bangert and K. Saarinen for advance copies of their works and Malcolm Heggie for discussions on platelets. L.H. thanks DTC for support.

- ¹A. T. Collins, H. Kanda, and H. Kitawaki, *Diamond Relat. Mater.* **9**, 113 (2000).
- ²D. Fisher and R. A. Spits, *Gems. Gemol.* **36**, 42 (2000).
- ³P. M. Martineau, S. C. Lawson, A. J. Lawson, S. J. Quinn, J. F. Evans, and M. J. Crowder, *Gems. Gemol.* **40**, 2 (2004).
- ⁴C. Clark, R. Ditchburn, and H. Dyer, *Proc. R. Soc. London* **237**, 75 (1956).
- ⁵J. N. Lomer and A. M. A. Wild, *Radiat. Eff.* **17**, 37 (1973).
- ⁶D. Twitchen, P. Martineau, and G. Scarsbrook, Patent Application WO 2004/022821, March 18 2004.
- ⁷R. Burns, D. Fisher, and R. Spitz, Patent Application WO 01/72406, April 04 2001.
- ⁸J. Walker, *Rep. Prog. Phys.* **42**, 1605 (1979).
- ⁹K. Iakoubovskii and G. Adriaenssens, *J. Phys.: Condens. Matter* **12**, 77 (2000).
- ¹⁰C. J. Fall, A. T. Blumenau, R. Jones, P. R. Briddon, T. Frauenheim, A. Gutiérrez-Sosa, U. Bangert, A. E. Mora, J. W. Steeds, and J. E. Butler, *Phys. Rev. B* **65**, 205206 (2002).
- ¹¹B. Willems, L. Nistor, C. Ghica, and G. VanTendeloo, 2005, presented at SBDD-X, LUC Belgium, February 2005.
- ¹²V. Avalos and S. Dannefaer, *Physica B* **340**, 76 (2003).
- ¹³J.-M. Mäki, V. Ranki, K. Saarinen, P. M. Martineau, and D. Fisher, 2005, presented at SBDD-X, LUC Belgium, February 2005.
- ¹⁴L. S. Hounscome, R. Jones, P. M. Martineau, M. J. Shaw, P. R. Briddon, S. Öberg, A. T. Blumenau, and N. Fujita, *Phys. Status Solidi A* **202**, 2182 (2005).
- ¹⁵R. Jones, B. J. Coomer, J. P. Goss, B. Hourahine, and A. Resende, in *Special defects in semiconducting materials*, Vol. 71 of *Solid State Phenomena*, edited by R. P. Agarwala (Scitech Publications Ltd., Zuerich-Uetikon, Switzerland, 2000). The interaction of hydrogen with deep level defects in silicon, pp. 173–248.
- ¹⁶C. Hartwigsen, S. Goedecker, and J. Hutter, *Phys. Rev. B* **58**, 3641 (1998).
- ¹⁷H. J. Monkhorst and J. D. Pack, *Phys. Rev. B* **13**, 5188 (1976).
- ¹⁸G. F. Bassani and G. Pastori Parravicini, in *Electronic states and optical transitions in solids*, Vol. 8 of *International series of monographs in the science of the solid state*, edited by R. A. Ballinger (Pergamon Press, Oxford, 1975).
- ¹⁹A. J. Read and R. J. Needs, *Phys. Rev. B* **44**, 13071 (1991).
- ²⁰V. Olevano, M. Palumbo, G. Onida, and R. Del Sole, *Phys. Rev. B* **60**, 14224 (1999).
- ²¹W. R. L. Lambrecht and S. N. Rashkeev, *Phys. Status Solidi B* **217**, 599 (2000).
- ²²L. X. Benedict, T. Wethkamp, K. Wilmers, C. Cobet, N. Esser, E. L. Shirley, W. Richter, and M. Cardona, *Solid State Commun. Rev. Lett.* **112**, 129 (1999).
- ²³*Landolt-Börnstein, new series*, edited by O. Madelung and M. Schulz (Springer, Berlin, 1989).
- ²⁴R. Q. Hood, P. R. C. Kent, R. J. Needs, and P. R. Briddon, *Phys. Rev. Lett.* **91**, 076403 (2003).
- ²⁵K. C. Pandey, *Phys. Rev. B* **25**, R4338 (1982).
- ²⁶T. G. Pedersen, *Phys. Rev. B* **67**, 113106 (2003).
- ²⁷V. Vorlíček, J. Rosa, M. Vaněček, M. Nesládek, and L. M. Stals, *Diamond Relat. Mater.* **6**, 704 (1997).
- ²⁸S. J. Charles, J. E. Butler, B. N. Feygelson, M. E. Newton, D. L. Carroll, J. W. Steeds, H. Darwish, C.-S. Yan, H. K. Mao, and R. J. Hemley, *Phys. Status Solidi A* **201**, 2473 (2004).
- ²⁹R. P. Chin, J. Y. Huang, Y. R. Shen, T. J. Chuang, H. Seki, *Phys. Rev. B* **52**, 5985 (1995).
- ³⁰J. P. Hirth and J. Lothe, *Theory of dislocations, Materials Science and Engineering* (McGraw-Hill, New York, 1968).
- ³¹J. Glinnemann, K. Kusaka, and J. Harris, *Z. Kristallogr.* **218**, 733 (2003).
- ³²U. Bangert, A. Harvey, M. Schreck, and F. Hoermann, *Phys. Status Solidi A* **202**, 2188 (2005).
- ³³J. Ristein, *Diamond Relat. Mater.* **9**, 1129 (2000).
- ³⁴X. Yu, D. Yang, X. Ma, J. Yang, L. Li, and D. Que, *J. Appl. Phys.* **92**, 188 (2002).
- ³⁵S. Sque, R. Jones, and P. Briddon, *Phys. Status Solidi A* **202**, 2091 (2005).
- ³⁶N. M. Johnson, F. A. Ponce, R. A. Street, and R. J. Nemanich, *Phys. Rev. B* **35**, R4166 (1987).
- ³⁷S. Muto, S. Takeda, M. Hirata, K. Fujii, and K. Ibe, *Philos. Mag. A* **66**, 257 (1992).